Moderate-Power Argon Microwave-Induced Plasma for the Detection of Metal Ions in Aqueous Samples of Complex Matrix

Peter G. Brown, David L. Haas, John M. Workman, and Joseph A. Caruso*

Department of Chemistry, University of Cincinnati, Cincinnati, Ohio 45221

Fred L. Fricke

U.S.F.D.A. Elemental Analysis Laboratory, 1141 Central Parkway, Cincinnati, Ohio 45202

Recent developments have shown microwave-induced plasma optical emission spectrometry (MIP-OES) to be compatible with direct solution introduction of aqueous samples. The present study was performed to further determine the effects of a complex sample matrix on the instrumental response of the moderate-power argon MIP. This was accomplished by examining the emission intensities of several metal ions, ranging in concentration from 10 ppb to 100 ppm, both in 2% HNO$_3$ solution and in synthetic ocean water (S.W.). To illustrate matrix effects, the sensitivity and linear dynamic range of each metal in 2% HNO$_3$ were compared with the same parameter in synthetic ocean water. Furthermore, to illustrate the application of this method to the analysis of real samples, NBS SRM bovine liver tissues were analyzed by moderate-power Ar MIP and by inductively coupled plasma (ICP) for comparison. It is shown here that the linear dynamic ranges obtained for many metals in complex solution matrices span 2 to 4 or more orders of magnitude and that the detection limits obtained with the MIP compare well with those of the more popular ICP. It is also shown that a complex sample matrix can lead to significant changes in sensitivity (enhancement and suppression). Finally, it is shown that both the MIP and the ICP performed well and were in agreement when used to analyze the NBS SRMs.

Over the past several years microwave-induced plasmas (MIP), operating with either argon or helium support gases, have become increasingly popular as sources for atomic emission (1–5). Until recently a major limitation of the MIP as an optical emission source has been its limited capability of accepting aqueous samples. The low-power (less than 100 W) microwave-induced plasmas found in many research laboratories are not effective at vaporizing, atomizing, and then exciting elemental emission from aqueous aerosols. To circumvent the problem of aqueous sample introduction, researchers have attempted alternate methods of sample introduction such as heating the aerosol followed by passage of the heated material through a condenser (6–8). This process eliminates much of the solvent from the sample but is cumbersome and has been found to suffer memory effects (7). Other researchers have attempted electrothermal vaporization methods for sample introduction which involves placing a small volume of aqueous sample on a tantalum or carbon substrate and electrothermally heating the sample to evaporate the solvent. This is followed by increased heating to vaporize the sample and introduce it into a carrier (or injection) gas stream of the plasma (9–12). Although these and other methods of sample introduction are available, few are as convenient to use as direct solution nebulization.

Several years ago Beenakker et al. (13) demonstrated that direct solution nebulization into a 150-W argon MIP sustained in a TM$_{010}$ resonant cavity was possible, and although the results were favorable, lower detection levels and freedom from matrix effects were available from the ICP (14).

Our experience with the standard TM$_{010}$ resonant cavity suggests that operating at powers above those used by Beenakker (13) are limited due to heating and eventual arcing within the commonly used external tuning stubs. Recently studies have appeared by the authors that describe a modified (internally tuned) TM$_{010}$ resonant cavity which allows significantly higher power operation (1, 2). Furthermore, spectroscopic temperature and electron density measurements of a 500-W Ar MIP (T_{rot} 3580 K, T_{exc} 14 200 K, N_e 2.6 × 10^{15}/cm^3) indicate that this cavity, operating at higher powers, is capable of producing a much more energetic plasma than the standard low-power externally tuned TM$_{010}$ cavity (15, 16). The significance of the above spectroscopic temperatures as well as fundamental plasma properties in general has been discussed in detail elsewhere (15–18). The internally tuned TM$_{010}$ cavity used to sustain the moderate-power (ca. 500 W) Ar MIP has been demonstrated to operate well with nebulized aqueous samples and yields detection limits comparable to those obtained by ICP-OES while operating with significantly lower power and gas flow rates (1, 2, 14, 19). The present study was performed to illustrate the utility of this Ar-MIP for the detection of metal ions in solution samples of complex matrix.

EXPERIMENTAL SECTION

Apparatus. The plasma described herein is sustained in an internally tuned TM$_{010}$ resonant cavity operated at 510-W forward power and 0-W reflected power. It should be noted that any reference to power refers to that measured at the generator. The actual power coupled to the plasma is unknown due to power losses, mainly as heat, in the microwave-transmission cable, connectors, and tuning stubs. This plasma has been operated at powers between 25 and 600 W, with 510 W used in this work for optimum signal-to-noise ratio (S/N).

The modified TM$_{010}$ cavity used in this work has been described in detail elsewhere (1) and will be only briefly reviewed here. The cavity consists of an 86.5 mm i.d. silver- and then gold-plated copper cylinder with variable (1, 2, or 3 cm) depth. Although previous studies (2, 20) have shown the 2-cm depth to yield slightly higher signal-to-noise ratios than either the 1- or 3-cm cavities, a depth of 1 cm was used in this work. Microwave energy at frequency 2450 MHz is coupled to the cavity through a coaxial transmission line which is attached to the coupling loop in the cavity as shown in Figure 1 of ref 2. The adjustable tuning stubs mounted on the cavity faceplate are used to control the tuning (impedance matching) of the plasma and are effective in reducing the reflected power to 0 W.

A schematic diagram of the entire solution analysis system is given in Figure 1. A complete list of the experimental components, including model numbers and manufacturers, is given in Table I. The compromise operating conditions used in this work are provided in Table II.

Procedure. To examine the effects of a complex sample matrix on the instrumental response of the moderate-power argon MIP,

Table I. Experimental Apparatus and Components

apparatus	model or size	manufacturer
microwave cavity	modified TM_{010}	laboratory
microwave generator	500 W, 2450 MHz	Micro Now
coaxial cable	50, 214 u Teflon	Andrews Corp.
tuning stubs	from 1878D stub tuner	Maury Microwave
discharge tube	8 mm o.d., 5 mm i.d.	McDanel Corp.,
(A) aluminum oxide	998	Beaver Falls, PA
(B) zirconium oxide	Z122	
monochromator	0.3 m focal length	McPherson Corp.
grating	1200 g/mm	McPherson Corp.
PMT	1P28	RCA
data collection	Intel 8088 microcomputer	laboratory built
amplifier	i to E	laboratory built
support gas	99.998% Ar	Wright Bros., Inc.

Table II. Operating Conditions of Spectrometric System

microwave frequency	2450 MHz
power (forward)[a]	510 W
power (reflected)	0 W
plasma viewing mode	axial
cavity depth	1.0 cm
argon flow rate	0.45 L/min
nebulizer	concentric
solution uptake rate	0.8 mL/min
slit widths	20 μm
discharge tube used[b]	alumina

[a] It should be noted that any reference made to power is that as measured at the generator. [b] Alumina was used for this experiment due to the unavailability of zirconium oxide tubes.

the detection limits, sensitivity, and the linear dynamic ranges of several metals in both synthetic ocean water and 2% nitric acid were compared. To examine these parameters, solutions of Cu, Mn, Ni, Zn, Fe, Cd, Au, and Cr as nitrates were prepared and serially diluted with either synthetic ocean water (S.W., 2.11% (w/v) NcCl, 0.41% (w/v) $MgCl_2$, 0.12% (w/v) $CaCl_2$, 0.08% (w/v) KCl, 0.4% (v/w) concentrated H_2SO_4) or 2% HNO_3. These metal ion solutions were then determined against their respective blank solutions (S.W. or 2% HNO_3) to obtain relative emission intensities and signal-to-noise ratios. The sample aerosol was generated through the use of a Meinhard C-2 concentric nebulizer and transported to the plasma through a conical spray chamber with impaction bead. A two-way software manipulated solenoid valve controller was used to simplify alternate introduction of the blank and sample solutions, thus eliminating the need for operator switching. The emission intensities from each solution (blank and then sample) were measured for 15 s. This was achieved by focusing the plasma image onto the entrance slit of a 0.3-m criss-crossed Czerny-Turner monochromator equipped with a 1200 g/mm grating. The position of the image was varied to yield maximum S/N for each element examined. An intermediate time delay between collection of the blank and the sample data was programmed to allow for equilibration of the spray chamber during each measurement. A current to voltage amplifier/filter was used to convert photocurrents generated at the photomultiplier into proportional voltages which were then digitized by a 16-bit analog-to-digital converter and passed to a laboratory-built Intel 8080 based microcomputer where all calculations were performed (2). Statistical detection limits were determined as the concentration of analyte which gave an instrumental response equal to three times the standard deviation of the background at the wavelength of interest. At least five replicates were determined for each data point in order to calculate the linear dynamic range, detection limit, and precision (relative standard deviation) in each case.

To illustrate the application of this method to the analysis of real samples, NBS SRM-1577 bovine liver tissues were analyzed for Cu and Fe by moderate-power argon MIP and by ICP for comparison. Two ICP's were utilized in this study. A Leeman
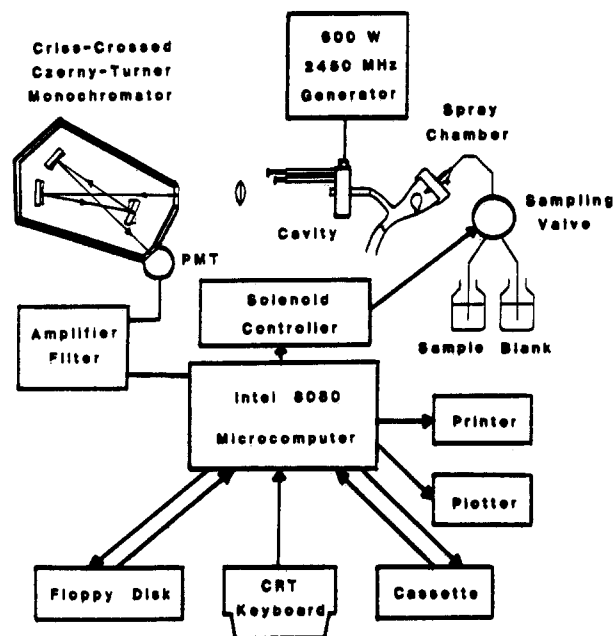

Figure 1. Experimental configuration.

Labs Plasma-Spec 2.5 was used in the university laboratories and a Jarrell-Ash Comp 1140 was used by the U.S. FDA Elemental Analysis Research Center for an independent analysis. The digestion precedures used for these tissues have been described previously (21). In this experiment, five replicate measurements were made of a matrix-matched blank (20% H_2SO_4, 100 ppm Ca, K, Mg, Na and P) and a matrix-matched 1 ppm iron and copper standard (20% H_2SO_4, 1 ppm Fe and Cu and 100 ppm Ca, K, Mg, Na, and P). These data were then used to establish the respective two-point calibration curves for iron and copper. Five replicate measurements were then made of the NBS bovine liver tissue, with a blank determination between each measurement, and the average of the five measurements was then compared to the respective calibration curve for the determination of iron and copper.

In addition to the solution studies performed, a brief examination of plasma-containment tubes was undertaken. The results may be useful to those interested in working with higher power microwave-induced plasmas. When an Ar MIP is operated at powers above 200 W, it is not practical to use a quartz discharge tube due to rapid degradation of the quartz. Aluminum oxide tubes have been found to function well at powers up to 600 W. However, they are rarely useful for more than a few days of operation due to rupture, from thermal shock, of the alumina. In this experiment, aluminum oxide was compared to yittria-stabilized zirconium oxide with respect to such qualities as ability to withstand the thermal shock of plasma ignition and contamination of the optical spectrum from metal oxide impurities in the tube material.

RESULTS AND DISCUSSION

Linearity and Detection Limits. By use of the experimental conditions given in Table II, linear ranges and detection limits have been determined for several metal ions in solution. Table III shows the detection limit, 3σ, obtained for each element in synthetic ocean water and in 2% nitric acid for comparison. Synthetic ocean water was selected as an appropriate matrix for this study because it resembles closely the matrix that is often found in biological samples and was thought to be appropriate for examination of matrix effects (suppressions, enhancements) commonly observed in emission spectrometry. A comparison of the detection limits reported for several elements by moderate-power Ar MIP, low-power Ar MIP, and inductively coupled plasma emission spectroscopy has appeared earlier (2). From these data and the data in ref 2, it can be noted that the moderate-power argon MIP is capable of producing detection limits that
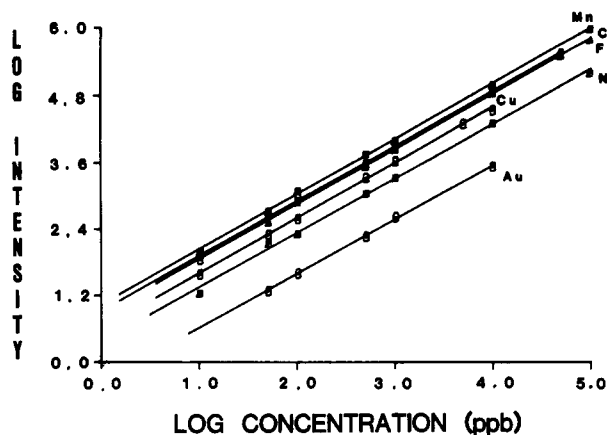
Figure 2. Linear dynamic ranges of several metal ions in S.W.

Table III. Detection Limits (DL) (3σ)(ng/mL) and Precision (Percent Relative Standard Deviation (% RSD)) of Metal Ions Determined in Both 2.0% HNO₃ and Synthetic Ocean Water (S.W.) Solutions

element	line, nm	DL in 2.0% HNO₃	% RSD	DL in S.W.	% RSD
Cu	324.7 I	5.2	3.2	2.3	1.9
	327.4 I[a]	1.7	2.0	1.2	0.80
Cr	425.4 I	3.3	0.5	5.0	0.6
	267.7 II[a]	12	7.8	160	19
Mn	403.1 I	3.9	2.8	1.5	3.6
	257.6 II[a]	1.4	1.4	40	16
Fe	372.0 I	3.6	0.70	3.5	2.2
	259.9 II[a]	4.1	1.4	290	8.5
Cd	228.8 I	1.0	0.60	1.7	1.6
	214.4 II[a]	4.6	3.6	36	35
Zn	213.9 I	2.3	0.60	1.2	1.9
	202.6 II[a]	7.4	1.7	93	36
Ni	341.5 I	6.7	1.0	7.3	1.1
	231.6 II[a]	30	1.5	30	20
Au	242.8 I	2.2	1.3	42.2	4.7

[a] Data from ref 2 for comparison.

compare favorable with those achieved with the ICP. It may be possible to attribute, in part, the low detection levels of this method to the greater residence time of analyte in the MIP. Analyte residence times on the order of 60 ms for the MIP are possible with a 5 mm i.d. discharge tube and 0.45 L/min or argon. Residence times for the ICP typically range from about 1 to 10 ms depending on the injector tube internal diameter and nebulizer gas flow rate.

Linear dynamic ranges have been calculated for each element analyzed; those for Mn, Cr, Fe, Cu, Ni, and Au are shown in Figure 2. This plot demonstrates that the response to Mn, Cr, Fe, and Ni is linear over at least 4 orders of magnitude, from 0.01 to 100 ppm (no extension beyond 100 ppm was attempted). It should be noted that for each linear range displayed, the best fit line has been extrapolated to the statistical detection limit of the respective element. The response to Au and Cu is linear over 2–3 orders of magnitude, from 0.50
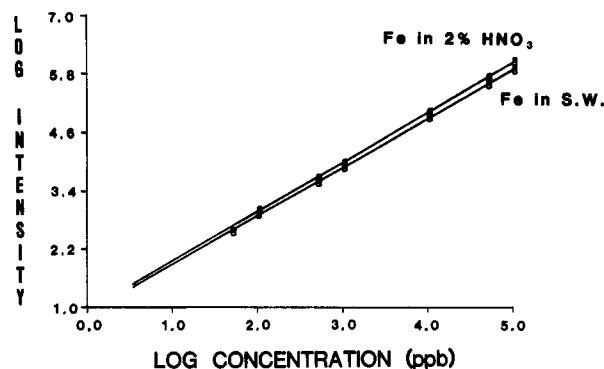

Figure 3. Comparison of the sensitivity for Fe in 2% HNO₃ and in S.W.
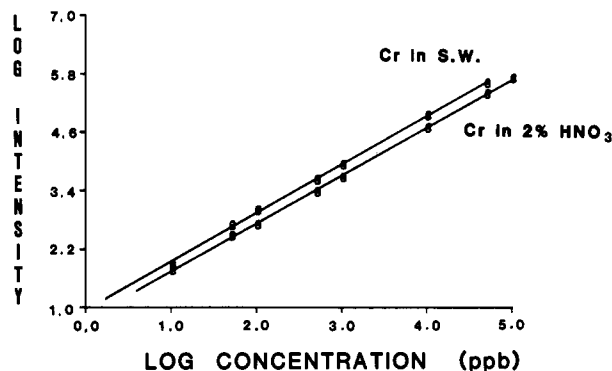

Figure 4. Comparison of the sensitivity for Cr in 2% HNO₃ and in S.W.

to 10 ppm and 0.01 to 10 ppm respectively. Statistical figures of merit for the log intensity vs. log concentration plots in Figure 2 are presented in Table IV. Both Cd and Zn yield instrumental responses linear over 2 orders of magnitude from 0.01 to 1 ppm. The shorter linear ranges for the latter four metals are due to self-absorption effects at high concentrations and may be compensated for by viewing plasma laterally (side-on) rather than axially. It has been shown that at least 1 order of magnitude gain in linearity can be achieved for Cu in 2% HNO₃ by lateral viewing of the plasma (2) which presents a more optically thin image of the plasma.

An important aspect of matrix effects on the instrumental response of any analytical technique is gathered from an examination of the sensitivity of the technique for a given analyte both with and without the presence of a complex sample matrix. For those elements in this study that were examined in both matrices (Au, Cr, Cu, and Fe), virtually all show some degree of suppression or enhancement in S.W. Figures 3 and 4 show log intensity vs. log concentration plots for Fe and Cr, respectively. Figure 3 demonstrates a slight sensitivity suppression for iron in S.W. In this case the emission intensity drops to 81% of the 2% HNO₃ value. Figure 4 demonstrates an 83% enhancement for Cr in S.W. over the intensity in 2% HNO₃. Further, copper shows a strong enhancement (113%) in S.W. and gold a factor of 50 suppression in S.W. Statistical figures of merit are provided for Figures 3 and 4 in Table V. It should be noted that atom line emission was used for the studies discussed above. In-

Table IV. Statistics for log–log Calibration Plots

element	slope	std dev of slope	intercept	std dev of intercept	corr coeff	linear range orders of magnitude
Mn	1.006	3.43 × 10⁻⁴	1.074	4.45 × 10⁻⁴	0.9932	4
Cr	0.998	2.15 × 10⁻⁴	0.939	3.28 × 10⁻⁴	0.9995	3.5
Fe	0.999	5.10 × 10⁻⁵	0.889	7.8 × 10⁻⁵	0.9999	4
Cu	1.037	7.0 × 10⁻⁵	0.675	9.4 × 10⁻⁵	0.9999	3
Ni	0.989	5.17 × 10⁻⁴	0.348	8.7 × 10⁻⁴	0.9989	4
Au	0.966	2.47 × 10⁻⁴	−0.589	2.75 × 10⁻⁴	0.9995	2.5

Table V. Statistics for Calibration Plots in 2% HNO₃ and Synthetic Ocean Water

element	matrix	slope	std dev of slope	corr coeff	intens at 1 ppm level ADC counts
Fe	2% HNO₃	1.020	4.6×10^{-5}	0.9999	9534
Fe	S.W.	0.999	5.1×10^{-5}	0.9998	7754
Cr	2% HNO₃	0.990	7.9×10^{-5}	0.9997	4673
Cr	S.W.	0.998	2.15×10^{-4}	0.9995	8564

Table VI. NBS SRM Analysis of BS SR7-1577 Bovine Liver by MIP and ICP

element	certified value, ppm	MIP, ppm	% RSD	% difference with certified	ICP,[a] ppm	% RSD	% difference with certified	ICP,[b] ppm	RSD	% difference with certified
Cu	1.27 ± 10%	1.37	1.4	8.08	1.34	2.3	5.7	1.3	ND[c]	4.2
Fe	2.29 ± 20%	2.21	1.9	3.67	2.36	4.0	2.9	2.6	ND	10.6

[a] Leeman Labs Plasma Spec ICP 2.5, university laboratories. [b] Jarrell Ash Atom Comp 1140 US FDA. [c] Not determined.

terestingly, Table III shows that when ion line emission is monitored, there is a large difference in detection limit and precision for any given element in the two solution matrices examined but that this is not the case when atom line emission is used.

The results of this study indicate that complex sample matrices do in the case of some metal ions alter the instrumental response of the moderate-power argon MIP when used for solution sample analysis. Though matrix effects are manifest most strongly when an analytical wavelength is chosen that corresponds to ion emission, suppressions and enhancements occur for atom lines as well. Strong suppression of ion emission is evidenced and thus results in a decrease in sensitivity and precision for analysis using those emission lines.

Table VI shows that both the MIP and the ICP were useful in accurately determining the levels of Cu and Fe in NBS bovine liver tissues. It is seen from Table VI that the MIP and ICP's agree to within the NBS tolerances with the certified values for both metals analyzed. This indicates that, though atom line suppressions and enhancements occur with the moderate-power Ar MIP, matrix-matched atom emission is nevertheless useful for accurately and precisely determining trace metal concentrations in real samples.

Plasma Containment. When elevated microwave powers are employed, the choice of discharge tube material becomes very important. The ideal discharge tube should contain the plasma without melting or cracking, allow easy centering of the plasma, and not introduce contaminants into the discharge. Quartz discharge tubes (mp 1610 °C), often used at lower power levels, melt at forward powers of between 200 and 250 W depending on tube size and flow rate of plasma gas. At some sacrifice of low flow rates, this may be somewhat alleviated by the tangential flow torches earlier described (2, 20). Aluminum oxide (mp 2075 °C) is superior to open tube quartz for use as a discharge tube; however, alumina tubes crack easily when rapidly heated and are rarely usable for more than a few days. Yittria-stabilized zirconium oxide (mp) 2700 ° C) is superior to alumina and quartz with respect to thermal

stability in that it does not crack or melt upon rapid heating and is reusable many times. The zirconia contains approximately 9% Y₂O₃ in its cubic crystal structure to stabilize it during periods of rapid heating and cooling. Both the Al₂O₃ and the ZrO₂ suffer drawback of containing several contaminants. The interfering elements found present in both tubes other than the obvious Al, Zr, and Y, were small amounts of Cu, Fe, K, Mg, Mn, and Na. The presence of these contaminating elements in the two types of discharge tubes increases the limits of detection and decreases the precision of this method for analysis for these elements. It is possible, however, to decrease the background level of these elements by soaking the tubes in 10% HNO₃ before using.

LITERATURE CITED

(1) Haas, D. L.; Carnahan, J. S.; Caruso, J. A. *Appl. Spectrosc*. **1983**, *37*, 82.
(2) Haas, D. L.; Caruso, J. A. *Anal. Chem*. **1984**, *56*, 2014.
(3) Skogerboe, R. K.; Coleman, G. N. *Anal. Chem*. **1976**, *48*, 611A.
(4) Zander, A. T.; Hieftje, G. M. *Appl. Spectrosc*. **1981**, *35*, 357.
(5) Carnahan, J. W. *Am. Lab. (Fairfield, Conn.)* **1983**, *15*(8), 31.
(6) Skogerboe, R. K.; Coleman, G. N. *Appl. Spectrosc*. **1976**, *30*, 504.
(7) Lichte, F. E.; Skogerboe, R. K. *Anal. Chem*. **1973**, *45*, 401.
(8) Kawaguchi, H.; Hasegawa, M.; Mizuike *Spectrochim. Acta, Part B* **1972**, *27B*, 205.
(9) Mitchell, D. G.; Aldous, K. M.; Canelli, E. *Anal. Chem*. **1977**, *49*, 1235.
(10) Carnahan, J. W.; Caruso, J. A. *Anal. Chim Acta* **1982**, *136*, 261.
(11) Kawaguchi, H.; Vallee, B. L. *Anal. Chem*. **1975**, *47*, 1029.
(12) Ng, K. C.; Caruso, J. A. *Appl. Spectrosc*. **1985**, *39*, 719.
(13) Beenakker, C. I. M.; Bosman, B.; Boumans, P. W. J. M. *Spectrochim. Acta, Part B* **1978**, *33B*, 373.
(14) Winge, R. K.; Peterson, V. J.; Fassel, V. A. *Appl. Spectrosc*. **1979**, *33*, 206.
(15) Brown, P. G.; et al. *Appl. Spectrosc*. **1986**, *40*, 477.
(16) Brown, P. G. et al. *Appl. Spectrosc*., in press.
(17) Greenfield, S.; McGeachin, H.; Smith, P. B. *Talanta* **1975**, *22*, 1.
(18) Marr, G. V. *Plasma Spectroscopy*., Elsevier: Amsterdam, 1968; Chapter 11.
(19) Haas, D. L.; Jamerson, J. D. *Spectrochim. Acta, Part B*, in press.
(20) Bolo-Kamara, A.; Codding, E. G. *Spectrochim. Acta, Part B* **1981**, *36B*, 973.
(21) Rader, J. I.; et al. *J. Nutr*. **1984**, *114*, 1946.